STUDIA UNIVERSITATIS BABEŞ-BOLYAI, CHEMIA, LIV, 4, 2009

SYNTHESIS, SPECTROSCOPIC AND ELECTROCHEMICAL CHARACTERIZATION OF A NEW CHROMIUM (III) SUBSTITUTED DAWSON POLYOXOMETALATE

**ADRIAN-RAUL TOMŞA[a], DANIELA CIOLOBOC[a], ANA MARIA TODEA[a,b],
RADU SILAGHI-DUMITRESCU[b], GRIGORE DAMIAN[c]
AND MARIANA RUSU[b]**

ABSTRACT. A new chromium (III) substituted Dawson 2-molybdo-15-tungsto-2-phosphate $K_7[Cr(H_2O)P_2Mo_2W_{15}O_{61}]\cdot 17H_2O$ was synthesized by reaction of Cr(III) chloride with monolacunary Dawson molybdo-tungsto-diphosphates $[P_2Mo_2W_{15}O_{61}]^{10-}$ in aqueous solution. The complex has been characterized using spectroscopic and electrochemical techniques. The FT-IR spectroscopic data indicate that the polyanion overall symmetry is restored after the coordination of Cr(III). Coordination of chromium (III) is further supported by the ^{31}P-NMR, EPR and UV-Vis electronic absorption spectroscopy results. Cyclic voltammograms of the chromium (III) complex exhibit three pairs of oxidation/reduction waves with negative $\varepsilon^{0`}$ values. These waves were assigned to two molybdenum-centered single electron redox processes and one tungsten-centered two electrons process. A positive shift of these waves when going from Dawson monolacunary complex to its Cr(III) complex. A modified Dawson structure was inferred from the results for the new chromium (III) complex, in which the chromium and molybdenum atoms are located to the same cap of the anion.

Keywords: polyoxometalate, Dawson structure, chromium, FT-IR spectroscopy, UV-Vis spectroscopy, NMR-spectroscopy, EPR-spectroscopy

INTRODUCTION

Polyoxometalates (POMs) comprise a rich and diverse family of metal-oxygen clusters of the early transition metals in high oxidation states, most commonly V(V), Mo(VI) and W(VI), with unique versatility in terms of shape, polarity, redox potentials, surface charge distribution, acidity, and solubility [1-4].

These compounds have promising applications in various domains, including catalysis [5,6], electrocatalysis [7], medicine [8,9], molecular conduction [10-12], magnetism [13], photochemistry [14,15], luminescence [16], analytical chemistry [17] and materials science [18].

---

[a] *"Babeş-Bolyai" University, "Raluca Ripan" Institute for Research in Chemistry, 30 Fântânele St., Cluj-Napoca, Romania, rtomsa@yahoo.com*

[b] *"Babeş-Bolyai" University, Faculty of Chemistry and Chemical Engineering, 11 Arany Janos St., RO-400028, Cluj-Napoca, Romania, mrusu@chem.ubbcluj.ro*

[c] *"Babeş-Bolyai" University, Faculty of Physics, 1 Mihail Kogălniceanu St., RO-400084, Cluj-Napoca, Romania*

The synthesis of polyoxometalates is mostly rather simple and straightforward, once the proper reactions conditions have been identified. However, the mechanism of formation of polyoxometalates is not yet well understood and is commonly described as self-assembly. Therefore, the design of novel polyoxometalates remains a challenge for synthetic chemists.

The most rational synthesis of new polyoxometalates uses the lacunary precursors prepared from the corresponding complete polyoxometalate species, by loss of one or more $\mathbf{MO_6}$ octahedra. Reaction of a stable lacunary polyoxometalate with transition metal ions mostly leads to a product in which the polyoxometalate framework remains unchanged.

For instance, under hydrolytic conditions, in the presence of Na_2CO_3, the α-$[P_2W_{18}O_{62}]^{6-}$ Dawson polyoxometalate loses three capping WO_6 octahedra, yielding a Dawson trilacunary polyoxotungstate derivative $[\alpha\text{-}P_2W_{15}O_{56}]^{12-}$ [19]. Furthermore, the reaction of the trilacunary derivative $[\alpha\text{-}P_2W_{15}O_{56}]^{12-}$ with molybdate, carried out in mild conditions, allows the selective addition of two molybdenum atoms in an apical site of $[\alpha\text{-}P_2W_{15}O_{56}]^{12-}$ [20]. Complexes of the resulting monolacunary Dawson polyanion, $[\alpha_2\text{-}P_2Mo_2W_{15}O_{61}]^{10-}$, with a first row transition metal cation are of particular interest for their electrocatalytic properties [21-23].

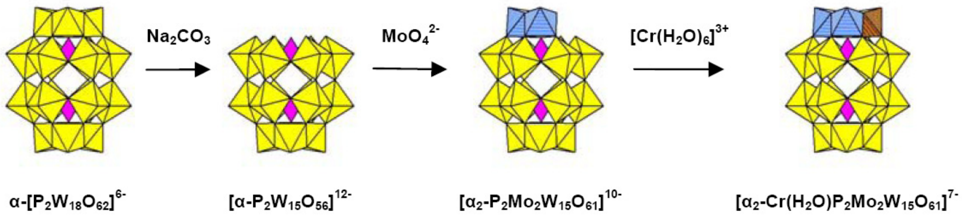

Figure 1. The preparation scheme of $\mathbf{\alpha_2\text{-}CrP_2Mo_2W_{15}}$.

Herein we report the synthesis, spectroscopic and electrochemical characterization of a new chromium (III) complex of Dawson monolacunary polyoxometalate $[\alpha_2\text{-}P_2Mo_2W_{15}O_{61}]^{10-}$, as aqueous soluble potassium salt. The $K_4Li_3[\alpha_2\text{-}Cr(H_2O)P_2Mo_2W_{15}O_{61}]\cdot 17H_2O$ complex ($\mathbf{\alpha_2\text{-}CrP_2Mo_2W_{15}}$) has been characterized by elemental and TG-DSC analysis, UV-Vis, FT-IR and ^{31}P-NMR spectroscopy, EPR, as well as by electrochemical measurements.

RESULTS AND DISCUSSION

The new chromium (III) polyoxometalate complex was synthesized in aqueous solution by reacting the potassium salt of the monolacunary Dawson polyoxometalate $K_{10}[\alpha_2\text{-}P_2Mo_2W_{15}O_{61}]\cdot 18H_2O$ ($\mathbf{\alpha_2\text{-}P_2Mo_2W_{15}}$) with chromium (III) chloride. In order to avoid the migration of molybdenum atoms, which may give numerous isomers, the synthesis must be performed in acidic solution heated to 40°C. Isolation of the products as potassium salts resulted in relatively good yields of the polyoxometalate complex.

The thermal stability of **α_2-CrP$_2$Mo$_2$W$_{15}$** was investigated by TG-DSC. The differential scanning calorimetry curve for **α_2-CrP$_2$Mo$_2$W$_{15}$** shows four endothermic and one exothermic processes in the region from 20°C to 650°C (Figure 2).

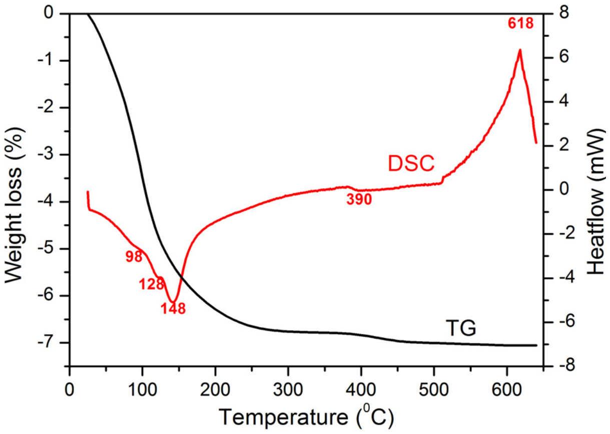

Figure 2. TG and DSC curves of **α_2-CrP$_2$Mo$_2$W$_{15}$**.

The three endothermic processes from ~25°C to 200°C are attributed to the desorption of 17 water molecules from the lattice structure. The endothermic process from ~380°C to 450°C is assigned to the loss of the coordination water molecule attached to Cr(III). The exothermic process observed from 500°C to 650°C coresponds to the collapse of the polyoxometalate framework. This assignement is also supported by FT-IR spectra, which show significant changes in the P-O and M-O (M= Mo, W) stretching modes after heating to 650°C (Figure 3).

The FT-IR spectrum of chromium (III) complex **α_2-CrP$_2$Mo$_2$W$_{15}$** in the P-O and M-O stretching region is shown in Figure 3, along with those of the monolacunary ligand **α_2-P$_2$Mo$_2$W$_{15}$** and complete Dawson polyoxometalate, $K_6[P_2W_{18}O_{62}]\cdot 14H_2O$ (**α-P$_2$W$_{18}$**).

As expected, in the FT-IR spectrum of the ligand **α_2-P$_2$Mo$_2$W$_{15}$**, the P-O vibration band, recorded between 1200 and 1000 cm^{-1}, is split, due to the decrease of the local symmetry. When Cr (III) fills the vacancy, the symmetry is restored. As a consequence, the FT-IR spectra of **α_2-CrP$_2$Mo$_2$W$_{15}$** and **α-P$_2$W$_{18}$** are similar. However, the spectrum of **α_2-CrP$_2$Mo$_2$W$_{15}$** exhibits an additional vibration band, recorded at 686 cm^{-1}, which was assigned to the stretching vibration $\nu_{(Cr\text{-}O)}$ [24,25].

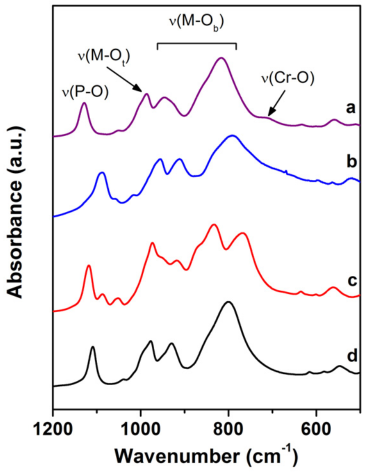

Figure 3. FT-IR spectra of **$\alpha_2\text{-CrP}_2\text{Mo}_2\text{W}_{15}$** (a), **$\alpha_2\text{-CrP}_2\text{Mo}_2\text{W}_{15}$** heated to 650ºC (b) **$\alpha_2\text{-P}_2\text{Mo}_2\text{W}_{15}$** (c) and **$\alpha\text{-P}_2\text{W}_{18}$** (d).

The vibrations in the 1000-700 cm^{-1} range were assigned to the asymmetric stretching of the bridges (M-O$_b$-M) and of the terminal bonds (M-O$_t$) [26]. Mention should be made of the fact that the stretching vibrations are shifted towards higher wavelengths, after the coordination of Cr(III), thus suggesting an increase of the polyoxoanion cohesion [26].

In the UV spectrum of **$\alpha_2\text{-CrP}_2\text{Mo}_2\text{W}_{15}$,** the two characteristic bands, assigned to the dπ-pπ charge transfer transitions M←O$_t$ and M←O$_b$ (M is Mo or W; O$_t$ is a terminal oxygen and O$_b$ is a bridging oxygen), were recorded at ~50000 cm^{-1} and ~35273 cm^{-1} [27, 28] (Figure 4a).

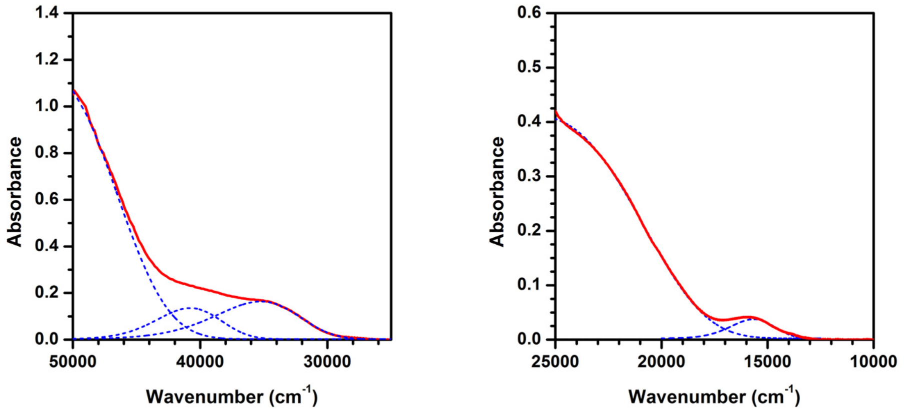

a b

Figure 4. The UV (a) and visible (b) electronic spectra of **$\alpha_2\text{-CrP}_2\text{Mo}_2\text{W}_{15}$** recorded in aqueous solution. The Gaussian components are represented with dashed lines.

The visible spectrum provides information about the local environment of Cr(III) (Figure 4b). Two bands characteristic of the chromium complexes, registered at 15650 cm^{-1} and 23446 cm^{-1} were assigned to $^4T_{2g}(F) \leftarrow {}^4A_{2g}(F)$ (v_1) and $^4T_{1g}(F) \leftarrow {}^4A_{2g}(F)$ (v_2) transitions, respectively. The v_3 band, assigned to $^4T_{1g}(P) \leftarrow {}^4A_{2g}(F)$ transition [29], overlaps the dπ-pπ charge transfer transitions $M \leftarrow O_t$ and $M \leftarrow O_b$ specific to the polyoxometalate structure, and appear as a shoulder at 40703 cm^{-1}. This assignment is supported by the calculation of the spectral parameters according to the method proposed by Lever (Dq= 1565 cm^{-1}, Dq/B=1.25, v_3/B=32.51, B=1252 cm^{-1}) [30].

While the ^{31}P-NMR of the ligand **α_2-$P_2Mo_2W_{15}$** shows a clean two-line spectrum with signals at -3.15 and -11.97 ppm, the spectrum of the Cr(III) complex **α_2-$CrP_2Mo_2W_{15}$** shows only a broadened peak at -11.58 ppm (Figure 5), which was assigned to P(2), the farthest phosphorus atom from the Cr(III) coordination site [31,32]. The phosphorus atom which is closest to the site of Cr(III) incorporation, P(1), was not observed probably because of the strong interaction with the paramagnetic ion.

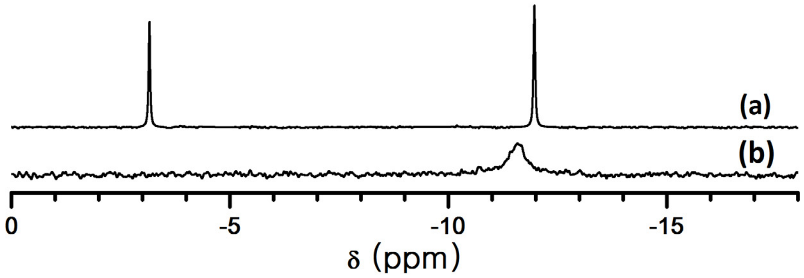

Figure 5. ^{31}P NMR spectra of **α_2-$P_2Mo_2W_{15}$** (a) and **α_2-$CrP_2Mo_2W_{15}$** (b), recorded in D_2O.

The EPR spectrum of **α_2-$CrP_2Mo_2W_{15}$** is shown in Figure 6. Low-temperature EPR spectra of other Cr(III)-substituted polyoxometalates reported before at 77K [24] show rhombic signals with features centered at 1500, 2000 and 3500 G, which are suggestive of a rhombohedrally distorted CrO_6 octahedron. Similarly, in our case, the low-field resonances in a range of g=3-6 indicate the presence of isolated Cr(III) species in orthorhombically distorted octahedral environments with S=3/2. The best fit of the simulated experimental spectrum at low field (1000-2000 G) was obtained assuming a Lorenzian line shape and two magnetic non- equivalent sites of chromium ions in a 0.55 to 0.45 ratio. The parameters for the first species were g_x= 5.11, g_y= 5.09, g_z= 5.0, and A_x= 251, A_y= 442, A_z= 494, which are characteristic of orthorhombically distorted symmetry. The parameters of the second species, g_x=4.1, g_y=3.53, g_z=3.22, and A_x=195, A_y=124, A_z=127, are characteristic of octahedral local symmetry [33]. These two magnetically- non-enequivalent species of Cr(III) are assigned to two different crystalline form of the polyoxometalate complex.

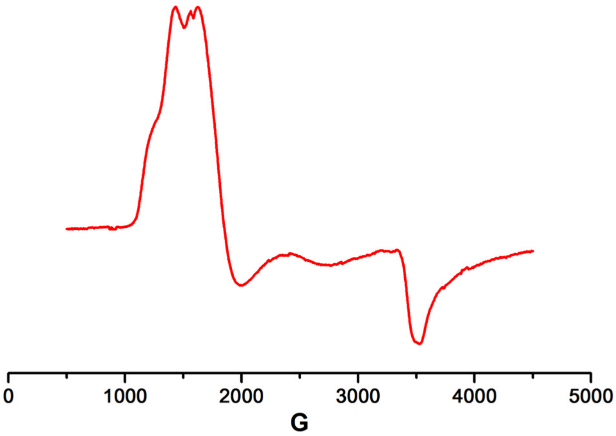

Figure 6. Low-temperature X-band EPR spectrum of **α_2-CrP$_2$Mo$_2$W$_{15}$**.

The electrochemical response of **α_2-CrP$_2$Mo$_2$W$_{15}$** in aqueous solution consists of three successive redox peak pairs in the negative potential range (Figure 7).

Peaks I and II were assigned to two molybdenum-centered single electron redox processes, while peak III corresponds to a two electrons tungsten-centered process [34]. The recorded cyclic voltammogram for the chromium (III) complex is very similar to those of **α_2-P$_2$Mo$_2$W$_{15}$**. Only a slight negative shift in the peak potentials was observed for **α_2-CrP$_2$Mo$_2$W$_{15}$** relative to the monolacunary ligand.

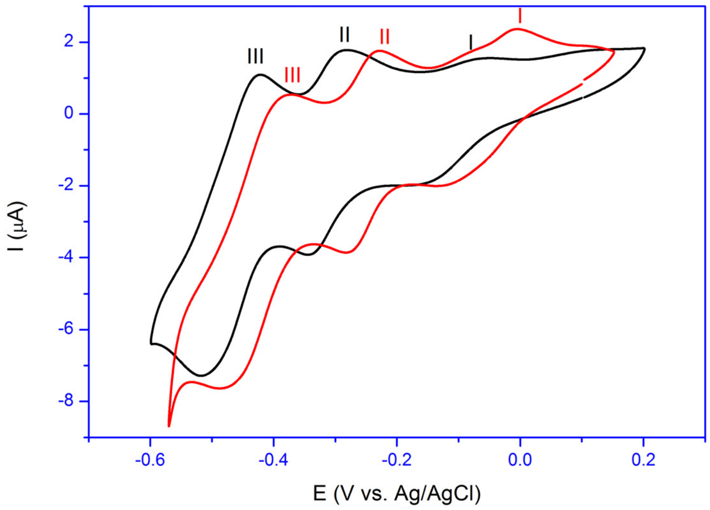

Figure 7. Cyclic voltammograms of **α_2-CrP$_2$Mo$_2$W$_{15}$** (black) and **α_2-P$_2$Mo$_2$W$_{15}$** ligand (red), recorded in 0.5 M HSO_4^- buffer solutions (pH= 3.0), sweep rate 10 mV s^{-1}.

Table 1. CV data for the chromium (III) complex and the parent Dawson monolacunary polyoxometalate.

Process	E_{pa} (V)	E_{pc} (V)	$\varepsilon^{0'}$ (V)	ΔE_p (V)
α_2-$P_2Mo_2W_{15}$				
I	-0.003	-0.102	-0.0525	0.099
II	-0.234	-0.279	-0.2565	0.045
III	-0.374	-0.485	-0.4295	0.111
α_2-$CrP_2Mo_2W_{15}$				
I	-0.052	-0.114	-0.0830	0.062
II	-0.287	-0.329	-0.3080	0.042
III	-0.419	-0.514	-0.4665	0.095

E_{pa}, oxidation potential; E_{pc}, reduction potential; $\varepsilon^{0'}$, formal standard potential estimated as the average of anodic and cathodic peak potentials; ΔE_p the difference between the redox peak potentials. Experimental conditions: 0.5 M HSO_4^- buffer solution; pH= 3.0, 25°C; glassy carbon working electrode; scan rate 10 mV s^{-1}; c=10^{-3} M, potentials recorded vs Ag/AgCl.

The formal standard potential $\varepsilon^{0`}$ (estimated as the average value of anodic and cathodic peak potentials) shows a negative shift with increasing values of pH (Figure 8a). For all three peaks, the $\varepsilon^{0`}$ versus pH dependences are linear, with slopes of 102.01 (I), 75.06 (II) and 73.96 (III) mV/ΔpH. The anodic to cathodic peak separation values (Δ*E*) and the described pH dependence are probably consistent with the fact that a single electron as well as one proton are involved in each redox process I and II, while two electrons and two protons are involved in the redox process III [32, 35-38].

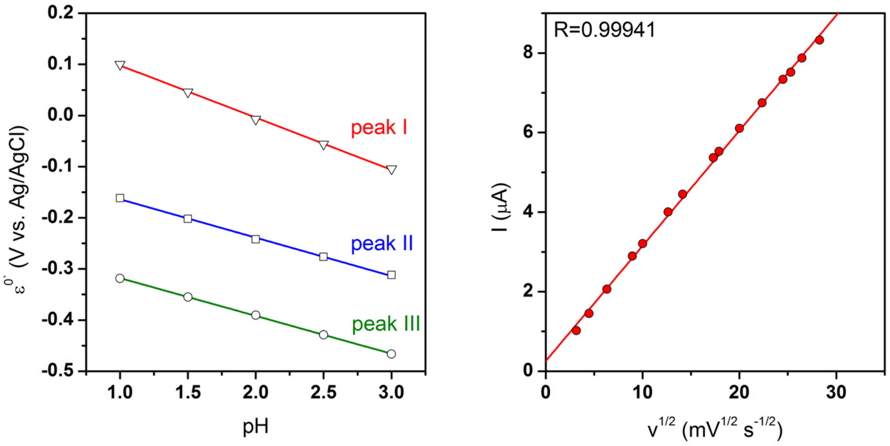

a

b

Figure 8. Dependence of the formal standard potentials on the pH for **α_2-$CrP_2Mo_2W_{15}$** (a); dependence of cathodic peak II current on the scan rate (b).

The linear relationship between peak currents and the square root of scan rates for cathodic peak II (Figure 8b) provides evidence for a diffusion controlled process [39].

CONCLUSIONS

The spectroscopic and electrochemical investigations of **α_2-CrP$_2$Mo$_2$W$_{15}$** provide evidence for the coordination of Cr(III) by the $[\alpha_2\text{-}P_2Mo_2W_{15}O_{61}]^{10-}$ Dawson monolacunary polyoxometalate. Both chromium and molybdenum atoms are located to the same cap of the anion. Cr(III) ion binds to five oxygen atoms, surrounding the vacancy of the ligand **α_2-P$_2$Mo$_2$W$_{15}$**, and to one water molecule. The electrochemical behavior of **α_2-CrP$_2$Mo$_2$W$_{15}$** illustrates the influence exerted by chromium upon the redox character of **α_2-P$_2$Mo$_2$W$_{15}$**. The redox behavior of the new chromium (III) derivative **α_2-P$_2$Mo$_2$W$_{15}$** recommends it as a promising mediator (electrocatalyst) in indirect electrochemical reactions.

EXPERIMENTAL SECTION

1. Materials

The monolacunary polyoxometalate $[P_2Mo_2W_{15}O_{61}]^{10-}$ was prepared according to the published method [19], starting from the Dawson polyoxometalate $[P_2W_{18}O_{62}]^{6-}$ (see Figure 1). The identity of precursors was established by ^{31}P-NMR and FT-IR spectra.

1.1. Preparation of $K_4Li_3[Cr(H_2O)P_2Mo_2W_{15}O_{61}]\cdot 17H_2O$

A sample of 1.33 g (5 mmol) of $CrCl_3\cdot 6H_2O$ was dissolved in 110 mL of molar acetic acid - lithium acetate buffer (pH=3.5), and 25.00 g (5.25 mmol) of $K_{10}[P_2Mo_2W_{15}O_{61}]\cdot 21H_2O$ was added with stirring. The mixture was heated at 40°C for 1 hour while the colour changed from green to brown, and then the clear solution was treated with 150 mL saturated KCl. The white precipitate was removed by filtration over a synthered glass frit and the brown filtrate was kept at 5°C. After three days, brown needle-like crystals appeared which were collected by filtration over a synthered glass frit, washed with ethanol and ether, and dried in air. Yield: 15 g (64.7%). Calcd. for $K_4Li_3[Cr(H_2O)P_2Mo_2W_{15}O_{61}]\cdot 17H_2O$: K 3.43, Li 0.46, Cr 1.14, P 1.36, Mo 4.30, W 60.70. Found: K 3.05, Li 0.40, Cr 1.12, P 1.44, Mo 4.05, W 62.08. FT-IR (cm^{-1}, KBr pellets, polyoxometalate region): 1093, 1014, 953, 912, 779, 686, 598, 565, 525, 476. ^{31}P NMR (D_2O, δ): -11.58 (s).

2. Methods

Elemental analysis was performed by inductively coupled plasma atomic emission spectroscopy on an ICP-OES Perkin Elmer Optima 3500 DV spectrometer. The water content was determined thermogravimetrically, with a METTLER-TOLEDO TG/SDTA 851 thermogravimeter (Pt crucible, 20 mL/min nitrogen flow, 5ºC/min heating rate).

A JASCO 610 FTIR spectrophotometer was used to record the FT-IR spectra (KBr pellets).

UV-Vis spectra were recorded on a Shimadzu UV-3101PC instrument using Teflon-stoppered quartz cells with a path length of 1 cm. A 10 μM aqueous solution of **α_2-CrP$_2$Mo$_2$W$_{15}$** was used to record the UV spectrum, while for the Vis spectrum was used a 1mM aqueous solution of **α_2-CrP$_2$Mo$_2$W$_{15}$**.

^{31}P-NMR spectra were recorded at 101.2561380 MHz using an ARX 250 spectrometer. Chemical shifts are reported in ppm using D_3PO_4 as external reference.

A Bruker EMX Micro spectrometer with a liquid nitrogen cooling system was employed for EPR spectra. Instrument conditions were: microwave frequency 9.43 GHz, microwave power 15.89 mW, modulation frequency 100 kHz, modulation amplitude 5 G, sweep rate 22.6 G/s; time constant 81.92 ms, average of three sweeps for each spectrum, temperature 100 K. To find the magnetic parameters, the experimental spectrum was simulated using the program POWFIT (http://epr.niehs.nih.gov/).

Electrochemical measurements were performed using a computer controlled AUTOLAB PGSTAT302N potentiostat. A conventional (single-compartment) three electrode electrochemical cell was used, with a Metrohm planar platinum counter electrode and a Metrohm Ag/AgCl reference electrode. Glassy carbon (Metrohm, Φ~ 3mm) was used as a working electrode (WE). This was polished with 0.3 μm alumina, followed by sonication for 3 min. in purified water before each run. The WE was polarized in a 10^{-3} M solution of the complex in 0.5 M HSO_4^- buffer (pH = 1.0 - 3.0) with a scan rate between 10 and 900 mV s^{-1}. Solutions were deoxygenated using purified N_2 gas (99.9%). While recording the voltammograms, N_2 was passed over the solution surface. All measurements were performed at room temperature.

ACKNOWLEDGMENTS

The authors gratefully acknowledge the financial support from the Romanian National Council for Scientific Research (PNCDI II - IDEI, Project No. 329/2007). We also thank Dr. Laura Elena Mureşan for TG-DSC measurements and Ioana Mihaela Perhăiță for elemental analysis.

REFERENCES

1. M.T. Pope, A. Müller (Eds.), "Polyoxometalates: From Platonic Solid to Antiretroviral Activity", Kluwer Academic Publishers, Dordrecht, **1994**.
2. M.T. Pope, A. Müller (Eds.), "Polyoxometalate Chemistry: From Topology via Self-Assembly to Applications", Kluwer Academic Publishers, Dordrecht, **2001**.
3. T. Yamase, M.T. Pope (Eds.), "Polyoxometalate Chemistry for Nano-Composite Design", Kluwer Academic Publishers, Dordrecht, **2002**.

4. J.J. Borrás-Almenar, E. Coronado, A. Müller, M.T. Pope (Eds.), “Polyoxometalate Molecular Science”, Kluwer Academic Publishers, Dordrecht, **2004**.
5. M. Misono, *Chemical Communications*, **2001**, 1141.
6. N. Mizuno, M. Misono, *Chemical Reviews*, **1998**, *98*, 199.
7. M. Sadakane, E. Steckhan, *Chemical Reviews,* **1998**, *98*, 219.
8. J.T. Rhule, C.L. Hill, D.A. Judd, *Chemical Reviews*, **1998**, *98*, 327.
9. T. Yamase, *Journal of Materials Chemistry*, **2005**, *15*, 4773.
10. E. Coronado, C. Giménez-Saiz, C.J. Gómez-García, S.C. Capelli, *Angewandte Chemie, International Edition,* **2004**, *43*, 3022.
11. E. Coronado, P. Day, *Chemical Reviews*, **2004**, *104*, 5419.
12. E. Coronado, C. Giménez-Saiz, C.J. Gómez-García, *Coordination Chemistry Reviews*, **2005**, *249*, 1776.
13. E. Coronado, J.R. Galán-Mascarós, C. Giménez-Saiz, C.J. Gómez-García, S. Triki, *Journal of American Chemical Society*, **1998,** *120,* 4671.
14. E. Papaconstantinou, *Chemical Society Reviews*, **1989**, *16*, 1.
15. A. Hiskia, A. Mylonas,E. Papaconstantinou, *Chemical Society Reviews*, **2001**, *30*, 62.
16. T. Yamase, *Chemical Reviews*, **1998**, *98*, 307.
17. D.P. Smith, M.T. Pope, *Analytical Chemistry*, **1968**, *40*, 1906.
18. D.E. Katsoulis, *Chemical Reviews*, **1998**, *98*, 359.
19. B.J. Hornstein, R.G. Finke, *Inorganic Chemistry*, **2002**, *41*, 2720.
20. M. Abbessi, R. Contant, R. Thouvenot, G. Hervé, *Inorganic Chemistry*, **1991**, *30*, 1695.
21. B. Keita, L. Nadjo, R. Contant, *Journal of Electroanalytical Chemistry,* **1998**, *443*, 168.
22. B. Keita, Y. Jean, B. Levy, L. Nadjo, R. Contant, *New Journal of Chemistry* **2002**, *26*, 1314.
23. B. Keita, Y.W. Lu, L. Nadjo, R. Contant, M. Abbessi, J. Canny, M. Richet, *Journal of Electroanalytical Chemistry*, **1999**, *477*, 146.
24. K. Wassermann, R. Palm, H.J. Lunk, J. Fuchs, N. Steinfeldt, R. Stösser, R., *Inorganic Chemistry*, **1995**, *34*, 5029.
25. K. Wassermann, H.J. Lunk, R. Palm, J. Fuchs, N. Steinfeldt, R. Stösser, R., M.T. Pope, *Inorganic Chemistry*, **1996**, *35*, 3273.
26. C. Rocchiccioli-Deltcheff, R. Thouvenot, *Spectrochimica Acta*, **1976**, *32A*, 587.
27. H. So, M.T. Pope, *Inorganic Chemistry*, **1972**, *11*, 1441.
28. A.R. Tomşa, D. Cioloboc, A.M. Todea, L. Mureşan, V. Paşcalău, M. Rusu, *Studia Universitatis Babeş-Bolyai, Seria Chemia*, **2009**, *LIV*, 33.
29. A.B.P. Lever, “Inorganic Electronic Spectroscopy”, Elsevier, New York, 2nd edn., **1984.**
30. A.B.P. Lever, *Journal of Chemical Education*, **1968**, *45*, 711.
31. D.K. Lyon, W.K. Miller, T. Novet, P.J. Domaille, E. Evitt, D.C. Johnson, R.G. Finke, *Journal of American Chemical Society*, **1991**, *113*, 7209.
32. C. Rong, F.C. Anson, *Inorganic Chemistry*, **1994**, *33*, 1064.

33. R.P.S. Chakradhar, J.L. Rao, G. Sivaramaiah, N.O. Gopal, *Physica Status Solidi (b)* **2005**, *242*, 2919.
34. M. Sadakane, E. Steckhan, *Chemical Review*, **1998**, *98*, 219.
35. S. Dong, X. Xi, M. Tian, *Journal of Electroanalytical Chemistry*, **1994**, *385*, 227.
36. X. Xi, G. Wang, B. Liu, S. Dong, *Electrochimica Acta*, **1995**, *40*, 105.
37. L. David, C. Crăciun, M. Rusu, O. Cozar, P. Ilea, D. Rusu, *Polyhedron*, **2000**, *19*, 1917.
38. A.R. Tomşa, L. Mureşan, A. Koutsodimou, P. Falaras, M. Rusu, *Polyhedron*, **2003**, *22*, 2901.
39. A.J. Bard, L.R. Faulkner, “Electrochemical Methods Fundamentals and Applications”, Wiley, New York, **2001**.